

Commission H (Waves in Plasmas) Activity Report

(Ver1.3)

March 10th, 2009

T. Okada and Y. Omura

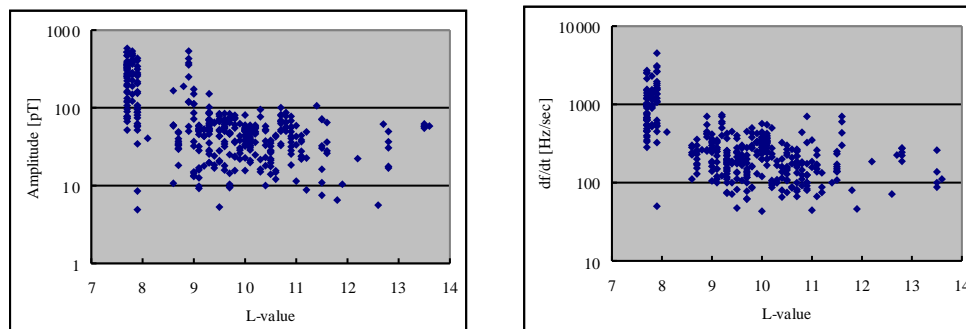
Research Topics

<Magnetospheric Observations>

GEOTAIL spacecraft has been operated since 1992. The Plasma Wave Instrument (PWI) is continuously collecting spectrum data and high time-resolution waveform data. It is expected to be in a good condition at least until the next long eclipse in 2009. The 24 hour plots of the observed wave spectrum data have been opened in the PWI web site <http://www.rish.kyoto-u.ac.jp/gtlpwi>, and <http://www.stp.isas.jaxa.jp/geotail>. Further, since 2005, the PWI team has started to open the access to all of 2 hour plots of the observed spectra. One can easily access the PWI 2 hour plots through the above web page.

The role of the PWI Principal Investigator has been taken over from Professor emeritus of Kyoto Univ. H. Matsumoto, who is the current president of Kyoto University to Dr. H. Kojima of Kyoto Univ.

Nagayama et al. [2008] analyzed the frequency sweep rates of rising chorus emissions. They performed the statistical analysis of chorus emissions observed by WFC onboard GEOTAIL from October 1992 to December 2007. Figure 1 shows the analytical results: (a) amplitudes vs. L values, and (b) frequency sweep rates vs. L values. Both chorus amplitudes and frequency sweep rates become smaller as the L-value becomes larger. This indicates that the frequency sweep rate would become large as the chorus wave amplitude grows, which is consistent with the simulation results reported by Hikishima et al. [2008a, b; 2009a].



(a) Amplitudes

(b) Frequency sweep rates

Figure 1: The amplitudes and frequency sweep rates of the chorus emissions depending on the L-value.

The mechanism for formation of the Earth's radiation belt has been an outstanding issue for utilization of the geospace environment. Kasahara et al. (2009) presented a typical magnetic storm event which occurred from 9 to 19 October, 1990, in which there is a clear correlation among continuous injection of hot electrons, generation of chorus, geomagnetic AE activity (all for ~8 days) and the acceleration of electrons to relativistic energies. They also showed the frequency characteristics of chorus elements that are important for non-linear wave particle interactions. They proposed a following scenario to explain the observations: the continuous injection of hot electrons associated with

the continuous AE activity. The hot electrons with $T_{\text{perp}}/T_{\text{para}} > 1$ temperature anisotropies excite whistler-mode chorus waves. The chorus interacts with energetic electrons accelerating them to MeV energies forming a flux of ‘killer electrons’ in the outer radiation belt.

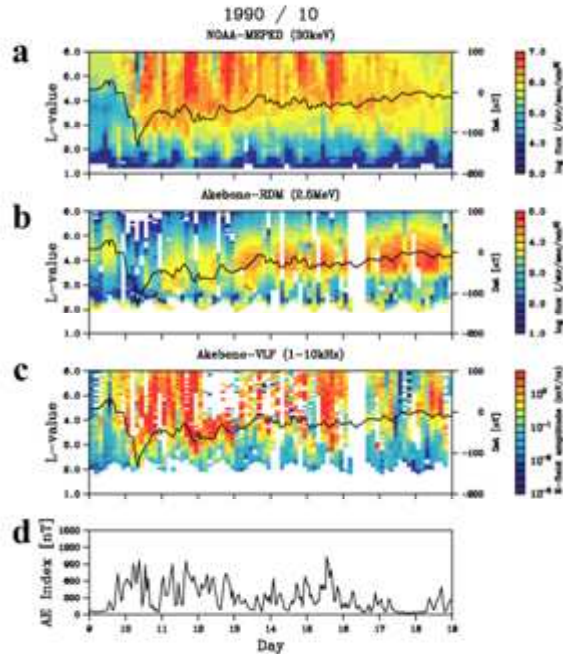


Figure 2:

Satellite and ground based data during the magnetic storm, October 1990: **a**, ~30 keV energetic electron fluxes measured by NOAA-10 from 9 to 19 October 1990. The Dst index is shown by a solid line. **b** and **c**, Relativistic ~2.5 MeV electron fluxes and intensity of 1-10kHz VLF waves observed by Akebono, respectively. **d**, The AE index during the magnetic storm

Knowledge of the characteristics of wire **antennas in space** plasmas used as sensors for electric field observations by scientific satellites in geospace is necessary to determine the absolute intensity and the phase of the electric field waves, because the observation data for the electric fields are available as voltage signals.

Akebono satellite was launched in 1989 to observe electromagnetic waves in geospace. Higashi et al. [2008] analyzed the data acquired from 1989 to 1995 for the antenna impedance measured by the vector impedance measuring instrument (VIP) for the electric field sensors onboard Akebono satellite. It was found that the resistance component of the antenna impedance has the frequency dependence.

By correcting the data of the antenna impedance measurement in consideration of the secular change of VIP, the resistance values became normal as shown in Figure 3 [Kamei and Higashi, 2008].

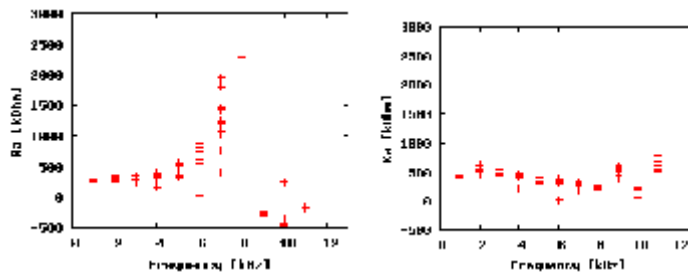


Figure 3: Correction of the resistance component of the antenna impedance (Left: Before correction, Right: After correction)

In Morioka et al. (2008), the dynamical behavior of **auroral kilometric radiation (AKR)** is investigated in connection with auroral particle acceleration at substorm onsets using high-time-resolution wave spectrograms provided by Polar/PWI electric field observations. AKR develops explosively at altitudes above a preexisting low-altitude AKR source at substorm onsets. This "AKR breakup" suggests an abrupt formation of a new field-aligned acceleration region above the preexisting acceleration region. The formation of the new acceleration region is completed in a very short time (amplitude increases 10,000 times in 30 seconds), suggesting that the explosive development is confined to a localized region. AKR breakups are usually preceded (1-3 minutes) by the appearance and/or gradual enhancement of the low-altitude AKR. This means that the explosive formation of the high-altitude electric field takes place in the course of the growing low-altitude acceleration. The development of the low-altitude acceleration region is thus a necessary condition for the ignition of the high-altitude bursty acceleration. The dH/dt component from a search-coil magnetometer at ground shows that a few minutes prior to substorm onsets, the quasi-DC component begins a negative excursion that is nearly synchronized with the start of the gradual enhancement of the low-altitude AKR, indicating a precursor-like behavior for the substorm. This negative variation of dH/dt suggests an exponentially increasing ionospheric current induced by the upward field-aligned current. At substorm onsets, the decrease in the quasi-DC variation of dH/dt further accelerates, indicating a sudden reinforcement of the field-aligned current.

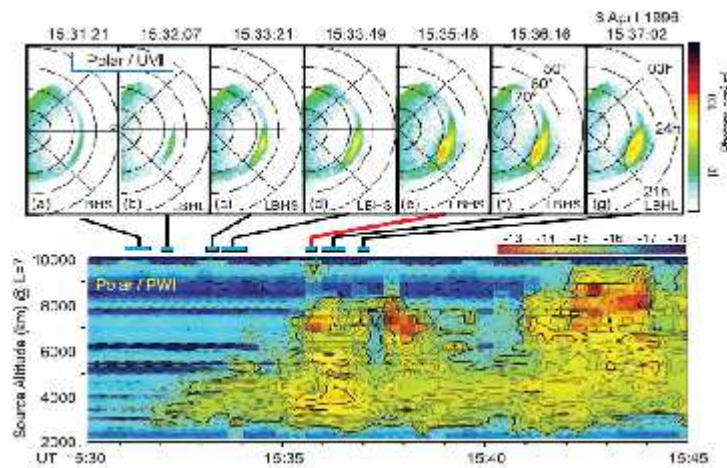


Figure 4. Relationship between global auroral activity and AKR development around a substorm onset. Upper panels: Polar/UVI images in dark hemisphere on 3 April 1996 showing an auroral breakup around 15:35 UT (image e). The small horizontal rectangles under images indicate exposure times. Lower panel: a-t diagram indicating AKR breakup at 15:35 UT after gradual enhancement of the low-altitude AKR.

Morioka et al. (2009) describes the onset process of auroral substorms in connection with the vertical evolution of auroral particle acceleration, on the basis of auroral kilometric radiation (AKR) dynamics. We show that the auroral acceleration process at substorm onset basically consists of two stages: (1) appearance/intensification of a low-altitude acceleration region at 4000–5000 km accompanied by initial brightening and (2) breakout of high-altitude field-aligned acceleration above the pre-existing low-altitude acceleration region at 6000–12 000 km, which is followed by auroral breakup and poleward expansion. It is also revealed that this two-stage evolution of auroral acceleration corresponds to the two-step reinforcement of field-aligned current.

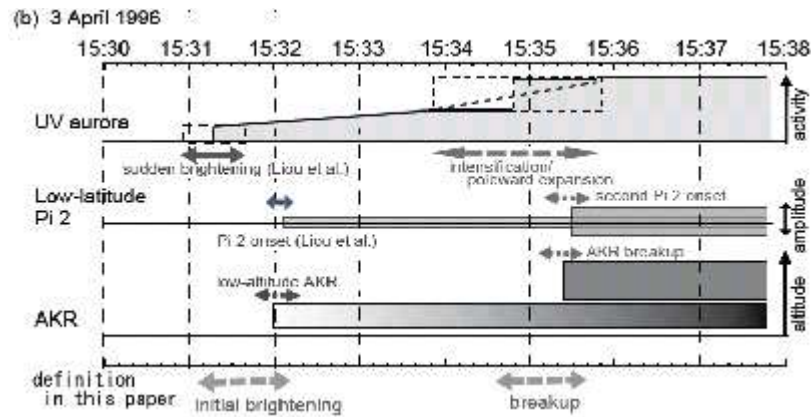


Figure 5. Schematic illustrations of time sequence for substorm on 3 April 1996. Vertical axes for UV aurora, Pi2, and AKR in each panel correspond to activity, amplitude, and altitude, respectively. Horizontal arrows indicate time tolerance for determining start time of each substorm step.

Miyoshi et al.(2008) showed for the first time evidence that electromagnetic ion cyclotron (EMIC) waves can cause the loss of relativistic electrons into the atmosphere. The process has been predicted theoretically since 1970's, but it has not been confirmed yet. Their conjunction observation from ground and satellite showed coincident precipitation of ions with energies of tens of KeV and of relativistic electrons into an isolated proton aurora. The coincident precipitation was produced by wave-particle interactions with EMIC waves near the plasmapause. The numerical calculation on the diffusion coefficients supported that the observed EMIC waves caused coincident precipitation of both ions in the ring current and relativistic electrons in the outer radiation belt.

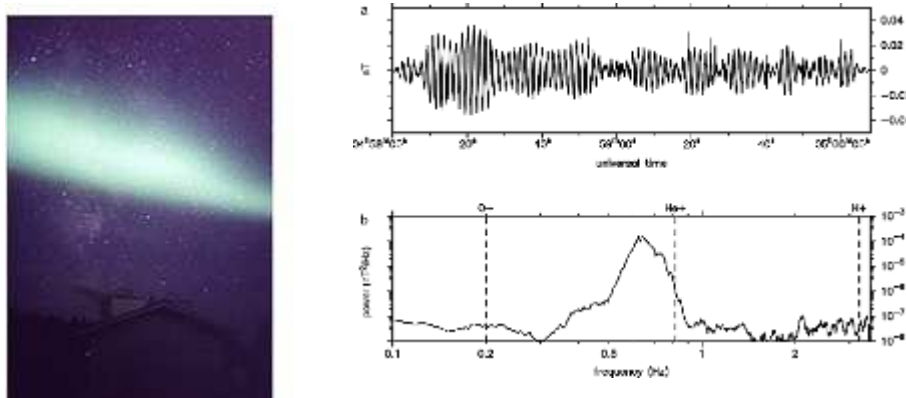


Figure 6 : (left) Photograph of isolated proton aurora in the southern sky of Athabasca, Canada, on September 5, 2005. Coincidence precipitations of both tens keV ions and relativistic electrons were observed inside this aurora. (right) Waveform of EMIC waves observed at Athabasca, when the isolated proton aurora was observed. Bottom panel indicates the power spectral density of EMIC waves. Helium-band EMIC waves are significantly detected.

Kitamura et al. (2008) have statistically studied meridional electron density distributions above 45 degree invariant latitude during geomagnetically quiet periods using the electron density data obtained from plasma waves observed by the Akebono satellite from March 1989 to February 1991, near solar maximum, in an altitude range of 274-10,500 km. They have found the largest seasonal variation and solar zenith angle (SZA) dependence of the electron density at an altitude of 2000 km with a factor of 50 in the trough, auroral and polar cap regions. The seasonal variation and SZA dependence are smaller, about a factor of 5-10, above 5000 km. Day-night asymmetries in each season are smaller than the seasonal variation. The scale height is larger in the dayside than in the nightside in each season. These results indicate that photoionization processes in the ionosphere strongly control electron density distributions up to at least 5000 km in the trough, auroral, and polar cap regions.

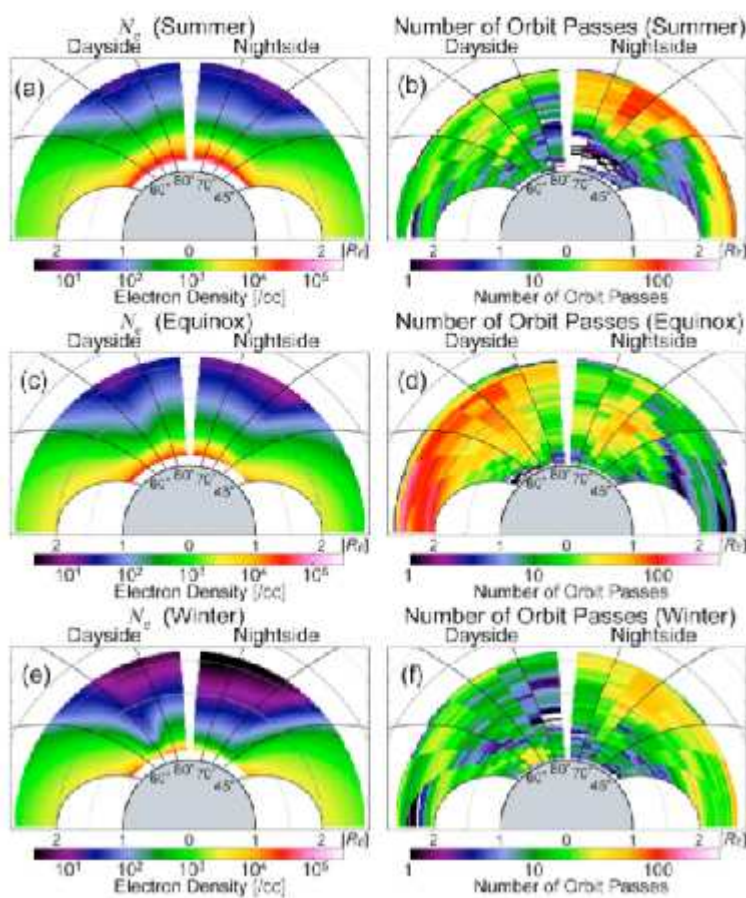


Figure 7: Electron density distribution models in a region of $ILAT > 45$ degree in an altitude range of 1000-10,500 km. Meridional electron density distribution models fitted by the sum of exponential and power law functions in the (a) summer, (c) equinox, and (e) winter seasons. The number of orbit passes in each bin are shown in the (b) summer, (d) equinox, and (f) winter seasons. The dipole magnetic field lines at $ILAT$ of 45, 60, 70, and 80 degree are shown in each panel.

CRRES electric field data during substorms have been analyzed by **Nishimura et al. (2008)** to investigate intense electric fields in the inner magnetosphere associated with dipolarizations. Substorm injections during 13:00 - 15:00 UT on 7 March 1991 exhibit many large-scale electric fields and short-duration electric field spikes. Large-scale electric fields with durations of 1 min are identified as spatial structures associated with the region 1 field-aligned currents. Amplitudes of electric fields reach 30 mV/m with a high correlation with variations of the magnetic field, and the Poynting fluxes are directed toward the ionosphere with magnitudes of more than 0.5 mW/m^2 . 16-Hz high-resolution data show intense electric field spikes with amplitudes of 100 mV/m^2 with durations of 1 s. Most of the spikes are electromagnetic with Poynting fluxes of 0.1 mW/m directed toward the ionosphere. The electric field spikes are identified as right-handed whistler waves with a size of 1000 km with frequencies just below the ion cyclotron frequency. A nearly simultaneous measurement by the DMSP-F9 satellite shows intense plasma flows with durations of 1 s and inverted-V electron precipitation. An estimation of the wave and particle energy fluxes shows that about half of the Poynting flux of the electric field spikes is consumed accelerating auroral particles, and 1% of the Poynting flux drives the fast plasma flows at the ionosphere. It is suggested that the electromagnetic spikes provide sufficient energy for auroral particle acceleration.

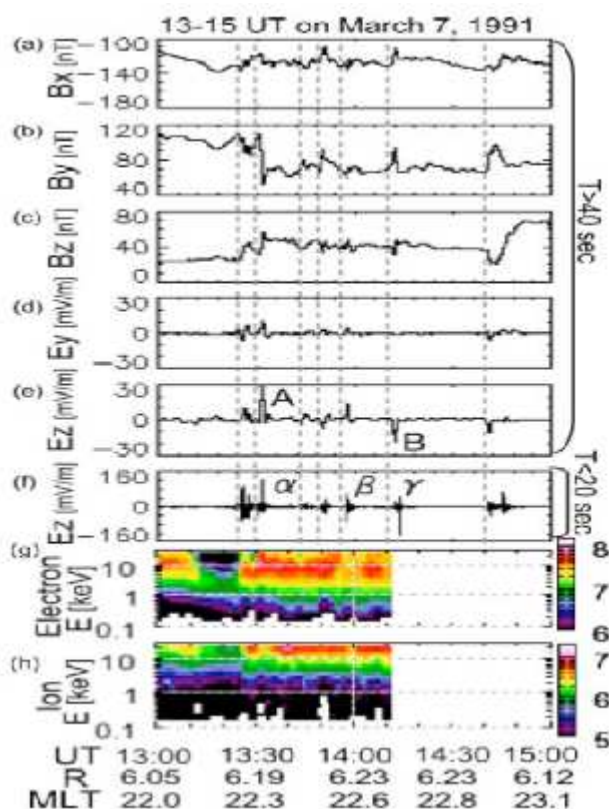


Figure 8: CRRES field and particle data between 13 and 15 UT on 7 March 1991. Figures a-c and d-e show low-pass filtered magnetic and electric field data. Figure 2f shows the high-resolution electric field with a period of less than 20 s. Figures g and h show the electron and ion energy flux. The intense electric fields labeled as A and B, and the spikes α , β , and γ have been analyzed by Nishimura et al. (2008).

Shiraishi et al. developed a automatic analyzer to measure the lower cut-off frequency of **Continuum Radiation (CR)**, which has been used to estimate an electron density around the Geotail spacecraft. So far, the lower cut-off frequency is detected by human's eyes, it takes a long time to obtain the lower cut-off frequency, and it is difficult to avoid subjective factors. In there study, they introduce a new scheme to detect the lower cut-off frequency of CR in signal analysis as shown in Figure 9. An example of such an analysis result is shown in Figure 10.

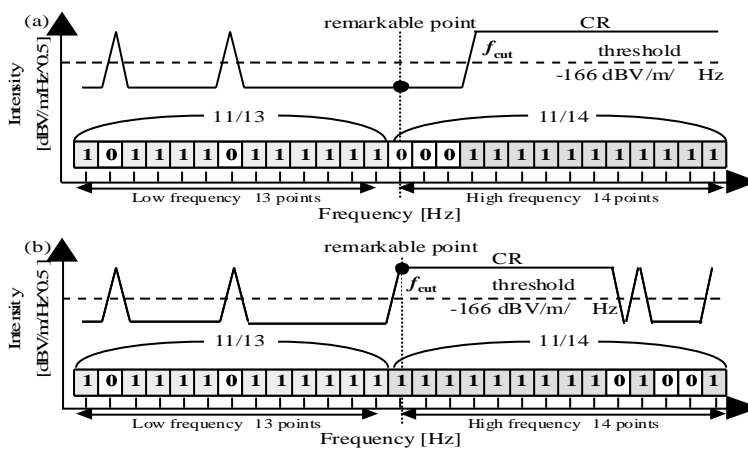


Fig.9 A new scheme to detect the lower cutoff frequency of CR. Examples of binarization process applied to model spectra: (a) A model spectrum which have a sequence of 「1」 away from the remarked frequency. (b) A model spectrum which have a sequence of 「1」 in the vicinity of the remarked frequency.

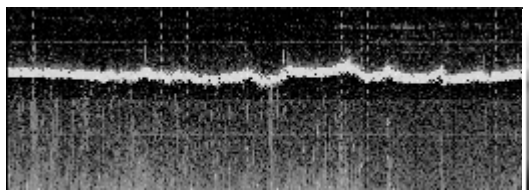


Fig.10 Detected cut-off frequencies at 10:00 UT – 12:00 Jan. 15, 1995.

<Jupiter Observations>

In Kimura et al. (2008), Ulysses had a “distant encounter” with Jupiter in February 2004. The spacecraft passed from north to south, and it observed Jovian radio waves from high to low latitudes (from +80° to +10°) for few months during its encounter. In this study, we present a statistical

investigation of the occurrence characteristics of Jovian quasi-periodic bursts, using spectral data from the unified radio and plasma wave experiment (URAP) onboard Ulysses. The latitudinal distribution of quasi-periodic bursts is derived for the first time. The analysis suggested that the bursts can be roughly categorized into two types: one having periods shorter than 30 min and one with periods longer than 30 min, which is consistent with the results of the previous analysis of data from Ulysses' first Jovian flyby [MacDowall, R.J., Kaiser, M.L., Desch, M.D., Farrell, W.M., Hess, R.A., Stone, R.G., 1993. Quasi-periodic Jovian radio bursts: observations from the Ulysses radio and plasma wave. Experiment. Planet. Space Sci. 41, 1059-1072]. It is also suggested that the groups of quasi-periodic bursts showed a dependence on the Jovian longitude of the sub-solar point, which means that these burst groups are triggered during a particular rotational phase of the planet. Maps of the occurrence probability of these quasi-periodic bursts also showed a unique CML/MLAT dependence. We performed a 3D ray tracing analysis of the quasi-periodic burst emission to learn more about the source distribution. The results suggest that the longitudinal distribution of the occurrence probability depends on the rotational phase. The source region of quasi-periodic bursts seems to be located at an altitude between 0.4 and 1.4 R_J above the polar cap region ($L > 30$).

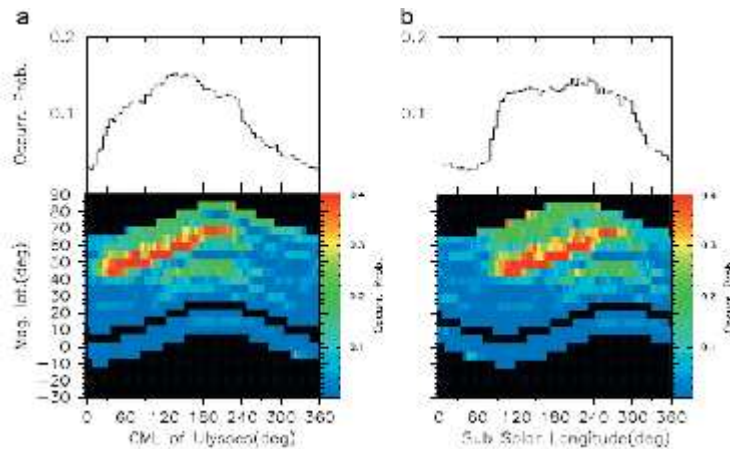


Figure 11. A map of occurrence probability of the QP burst groups. (a) The horizontal axis in each panel indicates the CML of Ulysses. The upper panel shows the CML distribution of the probability of the QP burst groups. The lower panel is the CML vs. the magnetic latitude map of the occurrence probability. The color indicates the occurrence probability. The black regions correspond to the lack of observation, whereas the blue regions indicate the lowest probability. (b) has a similar format to that of (a), but the horizontal axis is the sub solar longitude (SSL).

In Kimura et al. (2008b), Ulysses had a “distant encounter” with Jupiter when it was within 0.8 AU of the planet during February, 2004. The passage of the spacecraft was from north to south, and observations of the Jovian radio waves were carried out for a few months from high to low latitudes (+80° to +10°) of Jupiter. The statistical study performed during this “distant encounter” event provided the occurrence characteristics of the Jovian broadband kilometric radiation (bKOM), including the high-latitude component as follows: (1) the emission intensity of bKOM was found to have a sinusoidal dependence with respect to the central meridian longitude (CML), showing a broad peak at $\sim 180^\circ$, (2) bKOM was preferably observed in the magnetic latitudinal range from $\sim +30^\circ$ to $+90^\circ$, and the emission intensities at the high latitudes were found to be two times larger than that at the equatorial region, and (3) the emission intensity was controlled possibly by the sub solar longitude (SSL) of Jupiter. The intensity had a sharp peak around SSL $\sim 210^\circ$. A 3D ray tracing approach was applied to the bKOM in

order to examine the source distribution. It was suggested that: (1) the R-X mode waves generated through the Cyclotron Maser Instability process would be unable to reproduce the intense high-latitude component of the bKOM, (2) the L-O mode, which was assumed to be generated at frequencies near the local plasma frequency, was considered to be the dominant mode for past and present observations at mid- and high-latitudinal regions, and (3) the high-latitude component of bKOM was found to have a source altitude of 0.9–1.5 R_J (R_J: Jovian radii), and to be distributed along magnetic field lines having L > 10.

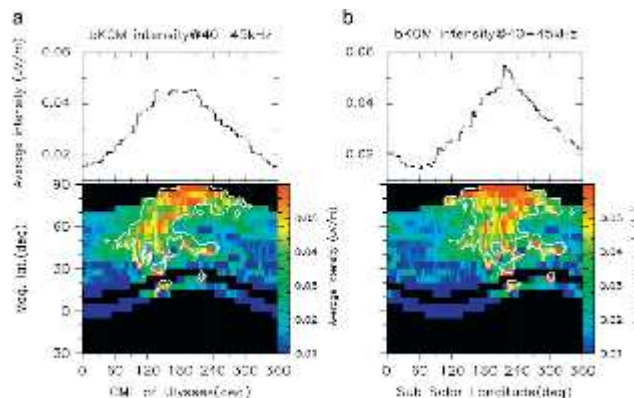


Figure 12. Intensity map of the bKOM. Horizontal axis in Fig. (a) indicates the CML of Ulysses as seen from Jupiter. Upper panel of Fig. (a) shows CML distribution of the average intensity. Lower panel of Fig. (a) depicts CML vs. magnetic latitude map of the average intensity. The color contours show integrated electric field intensity from 40–45 kHz. The white lines show the level of 0.035 mV/m. Fig. (b) is almost similar in format to that of Fig. (a), but for the horizontal axis, which shows the SSL.

< KAGUYA (SELENE) >

The purposes of the Lunar Radar Sounder (LRS) on-board the Kaguya (SELENE) spacecraft are (1) to perform radar sounding of the lunar subsurface structures which provide clues to understand the origin and evolution of the Moon, and (2) to observe natural radio waves from the Earth, Sun, and Jupiter and plasma waves associated with lunar wake and mini-magnetosphere due to crustal magnetic anomaly (Ono et al., 2008, Kumamoto et al., 2008, Kasahara et al., 2008).

LRS started the observation just after the extension of dipole antennas on Oct. 29. Through the operation from October 29, 2008 to September 10, 2008, 98 days worth of radar sounder data and 270 days worth of plasma wave data have been obtained.

Subsurface radar sounding of the Moon using LRS/SELENE

The Lunar Radar Sounder (LRS) on-board the Kaguya (SELENE) spacecraft started the lunar surface and subsurface soundings since November 2007 in order to understand the origin and evolution of the Moon. Kaguya is in circular orbit with an altitude of 100 km and an inclination of 90 degrees. Orbital period is about 2 hours. The LRS system transmits a radar signal modulated from 4 MHz to 6MHz with a pulse width of 200 microseconds and a peak power of about 800 Watts. The range resolution of LRS is 75 m in free space. The pulse repetition frequency of pulse transmission is 20Hz. After the operation for 10 month, the radar sounder observation covered almost whole area of the lunar

surface.

Ono et al. (2009) discovered prominent reflectors lying at the apparent depths of a few hundred meters in the nearside maria of the Moon. The age of subsurface layer can be determined by crater chronology of outcrop region. The prominent echoes found in Mare Selenitatis are probably from buried regolith layers accumulated during the depositional hiatus of mare basalts between 3.55 and 3.44 billion years ago. The mare ridges in the southern part of Selenitatis basin were formed after 2.84 billion years ago, which suggests that global cooling probably dominated the tectonics after 2.84 billion years ago.

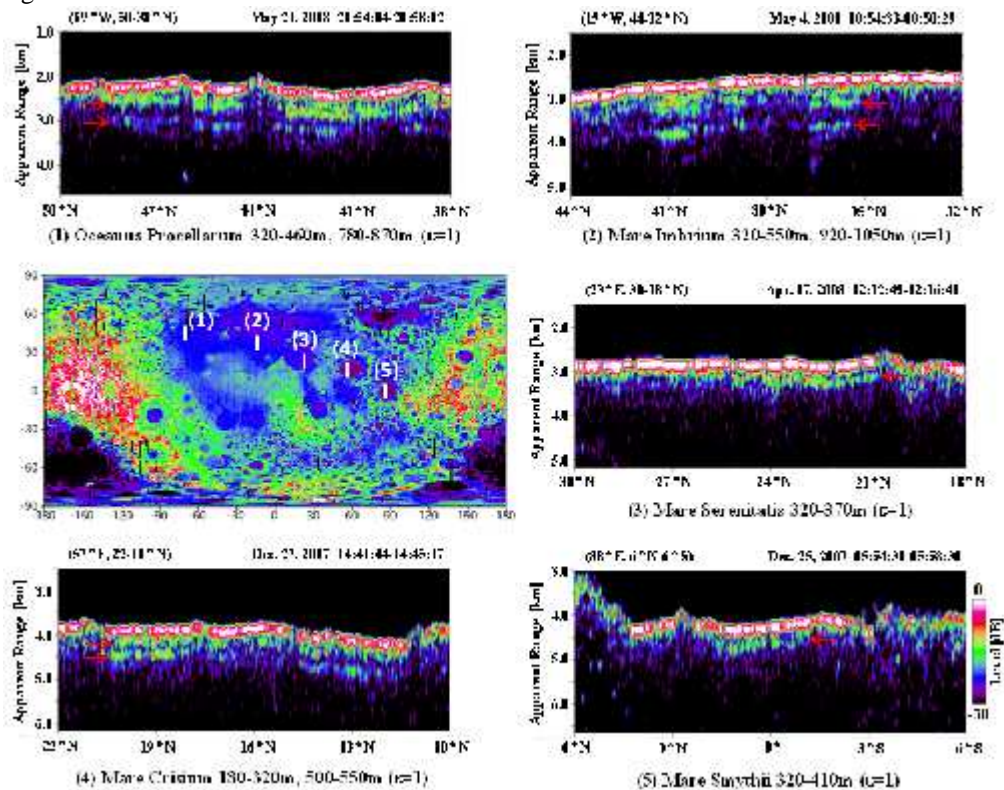


Fig. 13. Radargrams with obvious lunar subsurface echoes (red arrows). Observation ground tracks are plotted on the lunar topographic map of the Moon.

<Ionospheric Waves>

An Improved-Orion sounding **rocket SRP-5** has been carried out. The rocket was launched from the Poker Flat Research Range, Fairbanks, Alaska at 14:17 LT on January 10, 2009. The apex altitude is about 98 km at 150 seconds after launch. The primary science objective of SRP-5 Project ISIS (Ionospheric Science and Inertial Sensing) is to measure the plasma density structure of the high latitude D region ionosphere above Poker Flat Research Range. This will be accomplished using a plasma probe, radio receivers, and other sensors. The objective of TPU (Toyama Prefectural University) radio receiver is the investigation of the electron density profile in the high latitude D region at daytime. The electron density profile in the lowest ionosphere is estimated from the measured absorption of three radio waves (257 kHz, 660 kHz and 820 kHz) transmitted from navigation and broadcast stations near Fairbanks, Alaska.

Three signals were successfully observed from an altitude 0 km - 98 km during the ascent flight

(Figure 14 and Figure 15). The approximate electron density profile can be determined from the comparison between these experimental results and propagation characteristics calculated by the full wave method. Then the most probable electron density profile in the lowest ionosphere below 65 km will be demonstrated in future work.

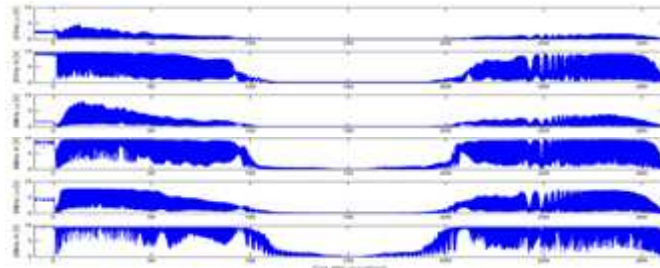


Figure 14 Measurement results of three radio wave intensities, 257 kHz ((a) Lo and (b) Hi), 660 kHz ((c) Lo and (d) Hi), and 820 kHz ((e) Lo and (f) Hi)

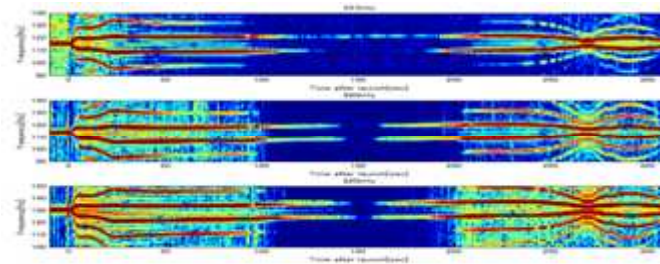


Figure 15 The spectrum from waveform measurement of 257 kHz (top panel), 660 kHz (middle panel) and 820 kHz (bottom panel).

<BepiColombo>

The BepiColombo is the science mission to Mercury. It is the first collaborative science mission between JAXA and ESA. The BepiColombo mission consists of two individual spacecraft called MPO (Mercury Planetary Orbiter) and MMO (Mercury Magnetospheric Orbiter). Scientists in Japan and Europe jointly proposed the plasma wave observation system called PWI (Plasma Wave Investigation) in the response to the AO (Announce of Opportunity) for MMO. The Principal Investigator of PWI is Prof. Hiroshi Matsumoto in Kyoto University, Japan. After reviewing the PWI proposal, the MMO Payload Review Committee in JAXA selected the PWI for the science payload onboard MMO spacecraft. The MMO launch is scheduled in 2014.

The PWI investigates plasma/radio waves and DC electric field in Mercury magnetosphere. It consists of two components of receivers, two sets of electric field sensors, two kinds of magnetic field sensors, and the antenna impedance measurement system.

The development and tests of the BBMs have been done by each PWI component team and the PWI has passed the Preliminary Design Review by JAXA, which was conducted in October, 2007. After that, the PWI team has moved to the phase of the development of the Engineering model (EM). The first EM tests of the PWI have been conducted from August to November, 2008 in Kyoto university. The tests have been conducted for both of the analogue parts and digital parts. Up to now, the PWI team has not found any serious problems. The second EM tests will start from April, 2009 in Kyoto university. After the second EM tests, the PWI will attend the EM system integration tests in JAXA, which is scheduled

in June, 2009.

<Polar Observations>

Ozaki et al. [2008a] analyzed the simultaneous ground-satellite observation of VLF waves in Antarctica, and discussed quantitatively the VLF penetration characteristics down through the polar ionosphere.

Ozaki et al. [2008b] estimated the polar ionospheric VLF exit point by using observation and full-wave calculation results to consider the effects of the magnetized ionosphere and of the Earth-ionosphere waveguide propagation. Firstly, to find the distinct exit point, they theoretically calculated the spatial distributions of the wave intensity and the polarization on the ground for VLF whistler mode waves coming down from the magnetized ionosphere. Then, they compared the calculated results with the observed data, to evaluate the plausible locations of the exit point for the auroral hiss events. Their results showed that the direction of the exit point for auroral hiss was found to be consistent with a bright aurora region, but the estimated exit point was located a few hundred kilometers equatorward of the associated aurora. Thus, they suggested that the ray paths for the auroral hiss could be different from the directions of the geomagnetic field lines for auroral particle precipitation.

Sato et al. (2008) have installed an Auroral Radio Spectrograph (ARS) system at Husafell station in Iceland in order to study the generation and propagation processes of MF auroral radio emissions, referred to as auroral roar and MF burst, in the polar ionosphere. In late 2006, the ARS detected one auroral roar and two MF bursts, which were identified as left-handed polarized waves. Results of data analysis, including other auroral data and particle spectra observed by the DMSP satellite, suggest that the MF bursts are generated by electrons with an average energy of several keV associated with auroral breakup. On the other hand, the auroral roar is generated as upper hybrid waves by relatively low-energy electrons over the observation site and propagates downward, being converted into L-O mode electromagnetic waves.

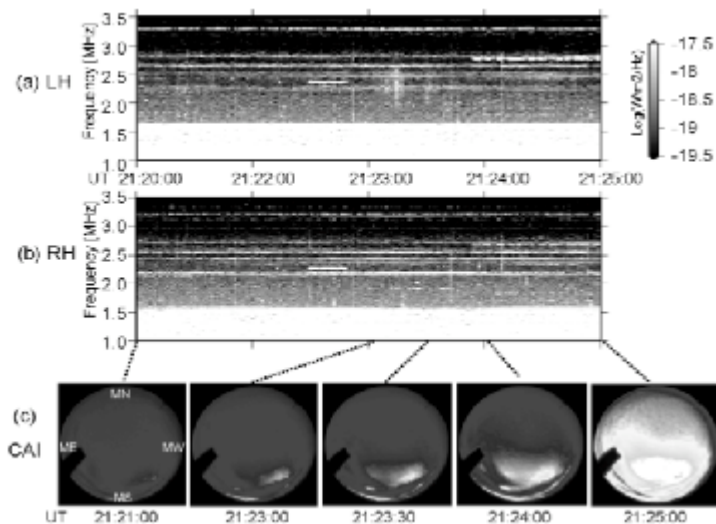


Figure 16: Dynamic spectra of LH (panel (a)) and RH (panel (b)) components of ARS data recorded 2121-2125 UT on September 23, 2006. The MF burst appeared at 2123:10 UT only in the LH component spectrum. The panel (c) shows a series of 427.8 nm auroral images recorded by the Conjugate Auroral Imager (CAI) instrument located at the Husafell station.

<ULF waves>

Miyoshi et al. (2008) used a unique set of ground and satellite observations to show evidence that left-hand polarised electromagnetic ion cyclotron (EMIC) waves near the plasmapause can precipitate relativistic electrons and lower-energy ions (with energies of tens of keV) at the same time into an isolated proton aurora. They backed up this interpretation by estimating the pitch angle diffusion coefficients for their event. Their study clarified that ions with energies of tens of keV affect the evolution of relativistic electrons in the radiation belts via cyclotron resonance with EMIC waves.

Maeda et al. (2009) selected 19 cases in which the Cluster spacecraft was located on the field line running through the midpoint of two ground magnetometer stations belonging to the CPMN (Circum-pacific Magnetometer Network), Tixie (TIK) and Chokurdakh (CHD), when TIK and CHD observed ULF waves caused by field line resonance (FLR). Then, for the 19 cases, they compared the electron density (N_e) observed by the WHISPER (Waves of High frequency Sounder for Probing the Electron density by Relaxation) instrument onboard the Cluster satellites with simultaneous plasma mass density (ρ) estimated from the FLR frequency observed by TIK and CHD, both corrected to the values on the magnetospheric equatorial plane along the same field line. As a result, the ratio of N_e to ρ fell into a realistic range for 15 out of the 19 events. It was also suggested that the contribution of heavy ions tends to increase when the magnetosphere is disturbed.

<Seismic ELF Emissions>

Ozaki et al. [2009] evaluated amplitude of a current moment (created by a seismic activity) in the conductive lithosphere from the viewpoint of possible detection of radiated waves with sensitivity of an electromagnetic sensor. They showed that if a seismic dipole source is larger than $1 \text{ kAm/Hz}^{1/2}$ placed at 10 km underground, we can detect it by a search coil magnetometer on the ground. However, even for the $1 \text{ kAm/Hz}^{1/2}$ dipole, we cannot observe it in the ionosphere. To detect it in the ionosphere, the current moment over $2.5 \text{ MAm/Hz}^{1/2}$ in the conductive medium of 10^{-3} S/m is required, which would not be a realistic value. Thus, they suggested that the direct observation of the seismic-related electromagnetic waves in the ionosphere would be quite difficult.

<Computer simulation>

The scattering process of energetic electrons by resonant interactions with whistler-mode chorus waves in the magnetosphere is examined in a self-consistent electromagnetic full-particle simulation [Hikishima et al., 2009b]. The coherent whistler-mode rising chorus can effectively scatter the energetic electrons through the cyclotron resonant interaction. With increasing the frequency of rising chorus, the distribution functions show a significant deformation along the decreasing resonance

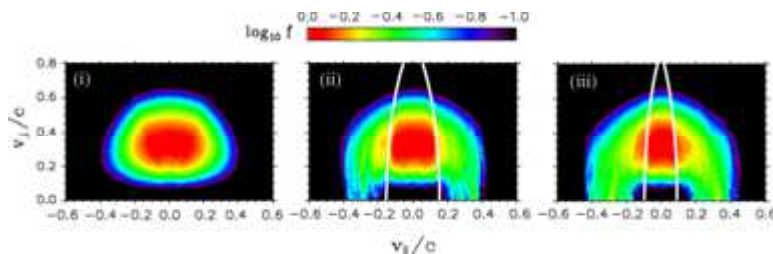


Figure 17: Temporal variation of distribution function of energetic electrons. The white curves are the resonance velocities.

velocity as shown with the elapsed times (i) to (iii) in Figure 17. The scattering of resonant electrons follows a nonlinear process. The nonlinear resonant interaction induces acceleration of trapped electrons and deceleration of untrapped resonant electrons. The nonlinear behavior of resonant electrons would contribute to the dynamics of magnetospheric electrons.

Katoh et al. (2008) have showed that in the simulation of **chorus** generation, some resonant electrons are rapidly energized by the processes of relativistic turning acceleration (RTA) and ultra-relativistic acceleration (URA). RTA and URA are particular forms of nonlinear wave trapping of resonant electrons by coherent whistler-mode waves and constitute viable mechanisms for the generation of relativistic electrons in the radiation belts of magnetized planets.

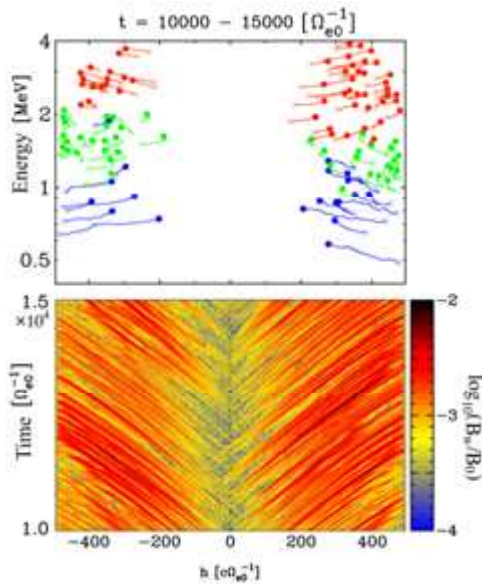


Figure 18: (Top) A fraction of resonant electrons are nonlinearly trapped by chorus waves and are effectively accelerated.

(Bottom) Wave packets of whistler-mode waves are successively generated near the magnetic equator, their amplitudes increasing as they propagate into both hemispheres.

Amano and Hoshino (2008) investigated electron acceleration mechanism in high Mach number collisionless perpendicular shocks in a weakly magnetized plasma using two-dimensional particle-in-cell simulations. They observe strong electron acceleration associated with large amplitude **electrostatic waves** in the shock transition region. Multidimensional effects as well as the self-consistent shock structure are essential for the strong electron acceleration at high Mach number shocks.

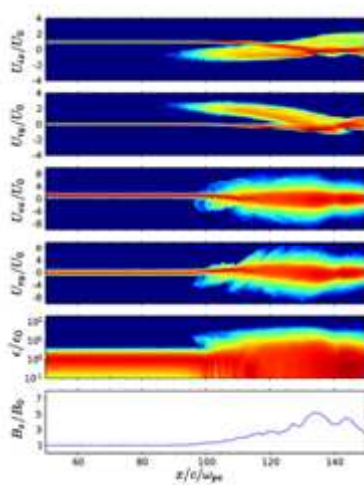


Figure 19: Snapshot of particle phase-space plots and compressional magnetic field profile averaged over the y-direction. Color represents the logarithm of the particle count in each bin. Note that the vertical scale of the electron energy spectrum (the second panel from the bottom) is shown on a logarithmic scale.

Saito et al.(2008) demonstrated two-dimensional electromagnetic particle-in-cell simulations in magnetized, homogeneous, collisionless electron-proton plasma to investigate the forward cascade of whistler turbulence. The turbulence displays magnetic energy spectra that are relatively steep functions of wavenumber and are anisotropic with more energy in directions relatively perpendicular to the background magnetic field than at the same wavenumbers parallel to it, as shown in Figure.

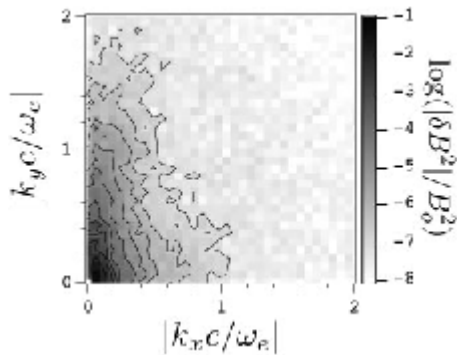


Figure 20: Magnetic fluctuation energy spectrum displaying the anisotropic turbulence. Bottom and left axis are wavenumbers parallel and perpendicular to the background magnetic field. The wavenumbers are normalized to electron inertial length. As shown in the figure 1, the fluctuating energy preferentially cascades to the perpendicular wavenumbers. Since obliquely propagating whistler wave tends to have electrostatic fluctuation, the whistlers preferentially heat electrons parallel to the background magnetic field through Landau resonance.

The anisotropic whistler turbulence is driven by Landau resonance on resonance, and heats them in directions both parallel and perpendicular to the background magnetic field, with stronger heating in the parallel direction. They show that whistler turbulence evolves preferentially to oblique propagation, and electrons gain more energy in the parallel direction.

<Antenna Characteristics in Space Plasma>

Miyake and Usui (2008) studied effects of photoelectron on the impedance characteristics of an electric field antenna by performing the electromagnetic Particle-In-Cell simulations. They modeled the photoelectron emission from the antenna surface and the antenna charging caused by the photoelectron emission. After an equilibrium solution of a photoelectron sheath profile is obtained, they examined the antenna impedance. They confirmed that the impedance characteristics in the presence of photoelectrons are well described by a parallel equivalent circuit consisting of the resistance and the capacitance.

Figure 7 shows the antenna conductance (inverse of the resistance) versus frequency for two cases of the photoelectron flux. The conductance value is greater for the case of the large photoelectron density. An analytical derivation of the antenna conduction shows that the conduction value is determined by the conduction current caused by the actual motion of photoelectrons. The result indicated that the antenna impedance can vary with the spacecraft spin, which causes the variation of the photoelectron density around the antenna.

They also developed a simulation method of analyzing the behavior of the plasma-wave receiving by an electric field antenna. The Langmuir or Whistler waves were set up as an initial condition, and the waves propagate in the simulation region. As a preliminary result, it was confirmed that the effective length of a simple dipole coincides with the half of its physical length in absence of sheath and photoelectron effects. They also confirmed that the effective length of MEFISTO aboard the BepiColombo is roughly equal to the distance between two separated sensor elements, which are deployed to the opposite directions.

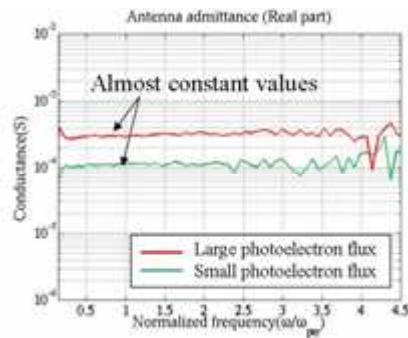


Figure 21: Antenna conductance as function of frequency for the cases of large and small photoelectron fluxes, which is obtained by the Particle-In-Cell simulations.

Imachi et al. [2008] have analyzed the impedance of the electric dipole antenna which is placed in the conductive medium such as space plasma at low frequencies. Their analysis is based on the result of Rheometry experiment to measure the relationship between the output voltage of a pair of dipole wire antennas and the intensity of the electric field applied to them in water. They investigated the equivalent circuits of this experiment assuming the electric field to be virtual power suppliers which are connected in parallel (see Figure 22), and found that the structure of the antenna including the insulation coating around the antenna wire affects the sensitivity at very low frequencies when it is connected to high impedance receivers. Additionally they performed computer simulation of the distribution of electric potential around the antenna wire, and clarified the difference in the distribution depending on the structure of the antennas (Figure 23).

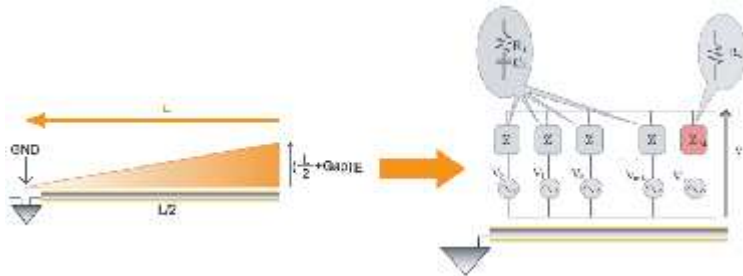


Figure 22: Equivalent circuit of an antenna wire, assuming the electric field to be virtual power suppliers which are connected in parallel.

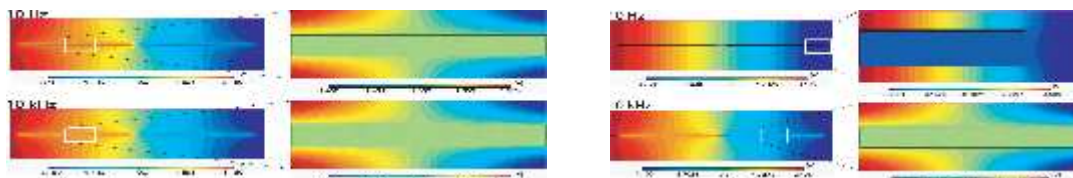


Figure 23: Simulated distributions of electric potential. The left figure shows the case that the antenna wires have no insulation coating. The right figure shows the case that they have insulation coating on the side of the wires.

References

- Amano, T., Hoshino, M., Electron shock surfing acceleration in multidimensions: Two-dimensional particle-in-cell simulation of collisionless perpendicular shock, *Astrophys. J.*, 690, 244, 2009
- Fujimoto A., Terumasa Tokunaga, Shuji Abe, Teiji Uozumi, Akimasa Yoshikawa, Kiyohumi Yumoto, and MAGDAS/CPMN Group, Global nature of Pc 5 magnetic pulsation during the WHI observation campaign, 124th SGEPS Fall Meeting, Sendai, Japan, Oct. 9-12, 2008.
- Hada, T. et al., Bi-spectrum analysis of MHD turbulence using multi-spacecraft data, ICPP2008, Sep.8-12, 2008, Fukuoka, Japan.
- Hada, T. et al., Transport of energetic particles in large amplitude MHD turbulence, ICPP2008, Sep.8-12, 2008, Fukuoka, Japan.
- Hasegawa, H., et al., Multi-scale structure of Kelvin-Helmholtz vortices detected at the earth's magnetospheric boundary, ICPP2008, Sep.8-12, 2008, Fukuoka, Japan.
- Higashi, R., M. Kamei, T. Imachi, and S. Yagitani, "The model for equivalent circuit of electric field sensor onboard satellite in space plasma," XXIXth URSI General Assembly, Chicago, USA, August, 2008.
- Hikishima, M., S. Yagitani, Y. Omura, and I. Nagano, "Full particle simulation of whistler-mode chorus emissions in the magnetosphere," 124th SGEPS Fall Meeting, Sendai, Japan, October, 2008a.
- Hikishima, M., S. Yagitani, Y. Omura, and I. Nagano, "Full particle simulation of whistler-mode chorus emissions in the magnetosphere," American Geophysical Union Fall Meeting, San Francisco, USA, December, 2008b.
- Hikishima, M., S. Yagitani, Y. Omura, and I. Nagano, "Full particle simulation of whistler-mode rising chorus emissions in the magnetosphere," *J. Geophys. Res.*, 114, A01203, doi:10.1029/2008JA013625, January, 2009a.
- Hikishima, M., S. Yagitani, Y. Omura, and I. Nagano, "Nonlinear scattering of magnetospheric electrons by chorus emissions in a full particle simulation," KDK symposium, Kyoto, Japan, March, 2009b. (in Japanese)
- Hirayama Y., Kiyohumi Yumoto, Teiji Uozumi, Akimasa Yoshikawa, and MAGDAS/CPMN Group, Nighttime and Daytime Equatorial Pi 2 Pulsations Observed at the MAGDAS/CPMN Stations, 124th SGEPS Fall Meeting, Sendai, Japan, Oct. 9-12, 2008.
- Ikeda A., Kiyohumi Yumoto, Manabu Shinohara, Teiji Uozumi, Akimasa Yoshikawa, and Kenro Nozaki, Observations of Pi 2 Ionospheric Electric Fields by FM-CW radars, 124th SGEPS Fall Meeting, Sendai, Japan, Oct. 9-12, 2008.
- Imachi, T., S. Yagitani, R. Higashi, and I. Nagano, "Estimation of the antenna impedance of the sensors aboard scientific spacecraft," 4 pages, XXIXth URSI General Assembly, Chicago, USA, August, 2008.
- Kamei, M., and R. Higashi, "The research on calibration for observation data of VLF plasma waves," 124th SGEPS Fall Meeting, Sendai, Japan, October, 2008.
- Katoh, Y., Y. Omura, and D. Summers, Rapid energization of radiation belt electrons by nonlinear wave trapping, *Ann. Geophys.*, 26, 3451--3456, 2008.
- Kasahara, Y., Y. Goto, K. Hashimoto, T. Imachi, A. Kumamoto, T. Ono, and H. Matsumoto, Plasma Wave Observation Using Waveform Capture in the Lunar Radar Sounder on board the SELENE Spacecraft, *Earth, Planets and Space*, 60, 341-351, 2008.
- Kasahara, Y., Y. Miyoshi, Y. Omura, O. P. Verkhoglyadova, I. Nagano, I. Kimura, and B. T. Tsurutani, Simultaneous satellite observations of VLF chorus, hot and relativistic electrons in a magnetic storm "recovery" phase, *Geophys. Res. Lett.*, 36(L01106), doi:10.1029/2008GL036454, 2009.
- Kawano, H., et al., Estimation of the magnetospheric plasma density from the ground by using ULF waves observed by MAGDAS/CPMN, ICPP2008, Sep.8-12, 2008, Fukuoka, Japan.
- Kawano H., Viacheslav Pilipenko, Satoko Takasaki, and Kiyohumi Yumoto, Improved hodograph method to identify field-line resonances in ground magnetometer data, 124th SGEPS Fall Meeting,

- Sendai, Japan, Oct. 9-12, 2008.
- Kimura, T., F. Tsuchiya, H. Misawa, A. Morioka, H. Nozawa, Radiation characteristics of quasi-periodic radio bursts in the Jovian high-latitude region, *Planet.Space Sci.*, 56, 1967–1976, 2008a.
- Kimura, T., F. Tsuchiya, H. Misawa, A. Morioka, and H. Nozawa, Occurrence and source characteristics of the high-latitude components of Jovian broadband kilometric radiation, *Planet. Space Sci.*, 56, 1155-1168, 2008b.
- Kitamura, N., A. Shinbori, Y. Nishimura, T. Ono, M. Iizima, and A. Kumamoto, Seasonal variations of the electron density distribution in the polar region during geomagnetically quiet periods near solar maximum, *J. Geophys. Res.*, 114, A01206, doi:10.1029/2008JA013288, 2009.
- Kumamoto, A., Ono, T., Kasahara, Y., Goto, Y., Iijima, Y., and Nakazawa, S., Electromagnetic compatibility (EMC) evaluation of the SELENE spacecraft for the lunar radar sounder (LRS) observations, *Earth Planets Space*, 60, 333-340, 2008.
- Maeda, N., S. Takasaki, H. Kawano, S. Ohtani, P. M. E. Decreau, J. G. Trotignon, S. I. Solov'yev, D. G. Baishev, and K. Yumoto, Simultaneous observations of the plasma density on the same field line by the CPMN ground magnetometers and the Cluster satellites, *Advances in Space Research*, doi:10.1016/j.asr.2008.04.016, 43(2), 265-272, 2009.
- Matsukiyo, S. and T. Hada, Relativistic particle acceleration in developing Alfvén turbulence, *ICPP2008*, Sep.8-12, 2008, Fukuoka, Japan.
- Miyoshi, Y., K. Sakaguchi, K. Shiokawa, D. Evans, J. Albert, M. Connors, and V. Jordanova, Precipitation of radiation belt electrons by EMIC waves, observed from ground and space, *Geophys. Res. Lett.*, 35, L23101, doi:10.1029/2008GL035727, 2008.
- Miyoshi, Y., K. Sakaguchi, K. Shiokawa, D. Evans, J. Albert, M. Connors, and V. Jordanova (2008), Precipitation of radiation belt electrons by EMIC waves, observed from ground and space, *Geophys. Res. Lett.*, 35, L23101, doi:10.1029/2008GL035727.
- Morioka, A., Y. Miyoshi, F. Tsuchiya, H. Misawa, K. Yumoto, G. K. Parks, R. R. Anderson, J. D. Menietti, E. F. Donovan, F. Honary, and E. Spanswick, AKR breakup and auroral particle acceleration at substorm onset, *J. Geophys. Res.*, 113, doi:10.1029/2008JA013322, 2008.
- Morioka, A., Y. Miyoshi, F. Tsuchiya, H. Misawa, K. Yumoto, G. K. Parks, R. R. Anderson, J. D. Menietti, and F. Honary, Vertical evolution of auroral acceleration at substorm onset, *Ann. Geophys.*, 27, 525-535, 2009.
- Miyake, Y., and H. Usui, Analysis of Photoelectron Effect on the Antenna Impedance via Particle-In-Cell Simulation, *Radio Science*, VOL. 43, RS4006, doi:10.1029/2007RS003776, 2008.
- Nagayama, M., M. Hikishima, S. Yagitani, I. Nagano, and H. Matsumoto, "Generation and propagation of chorus emissions observed in the magnetosphere," 124th SGEPS Fall Meeting, Sendai, Japan, October, 2008.
- Nariyuki, Y., Stabilization of electromagnetic ion beam instabilities by finite amplitude Alfvén waves revisited, *ICPP2008*, Sep.8-12, 2008, Fukuoka, Japan.
- Nariyuki, Y., et al., A comprehensive model on parametric instabilities of Alfvén waves in the solar wind *ICPP2008*, Sep.8-12, 2008, Fukuoka, Japan.
- Nishimura, Y., J. Wygant, T. Ono, M. Iizima, A. Kumamoto, D. Brautigam, and F. Rich, Large-amplitude wave electric field in the inner magnetosphere during substorms, *J. Geophys. Res.*, 113, A07202, doi:10.1029/2007JA012833, 2008.
- Ono, T., A. Kumamoto, Y. Yamaguchi, A. Yamaji, T. Kobayashi, Y. Kasahara, and H. Oya, Instrumentation and Observation Target of the Lunar Radar Sounder (LRS) Experiment on-board the SELENE Spacecraft, *Earth, Planets and Space*, 60, 321-332, 2008.
- Ono, T., A. Kumamoto, H. Nakagawa, Y. Yamaguchi, S. Oshigami, A. Yamaji, T. Kobayashi, Y. Kasahara, H. Oya, Lunar radar sounder observations of subsurface layers under the nearside maria of the Moon, *Science* 13, 323, 909-912, doi:10.1126/science.1165988, 2009.
- Ozaki, M., S. Yagitani, I. Nagano, Y. Hata, H. Yamagishi, N. Sato, and A. Kadokura, "Polar ionospheric

- penetration characteristics of down-going whistler mode waves by multipoint ground-based and satellite observations,” 4 pages, XXIXth URSI General Assembly, Chicago, USA, August, 2008a.
- Ozaki, M., S. Yagitani, I. Nagano, Y. Hata, H. Yamagishi, N. Sato, and A. Kadokura, “Localization of VLF ionospheric exit point by comparison of multipoint ground-based observation with full-wave analysis,” *Polar Science*, Volume 2, Issue 4, pp.237-249, December, 2008b.
- Ozaki, M., S. Yagitani, I. Nagano, K. Miyamura, “Ionospheric penetration characteristics of ELF waves radiated from a current source in the lithosphere related to seismic activity,” *Radio Science*, 44, RS1005, doi:10.1029/2008RS003927, February, 2009.
- Sato, Y., T. Ono, M. Iizima, A. Kumamoto, N. Sato, A. Kadokura, and H. Miyaoka, Auroral radio emission and absorption of medium frequency radio waves observed in Iceland, *Earth Planets Space*, 60, 207-217, 2008.
- Saito, S., S. P. Gary, H. Li, and Y. Narita. Whistler turbulence: Particle-in-cell simulations. *Phys. Plasmas*, 15:102305, 2008.
- Shiraishi, T., K. Ishisaka, T. Miyake, T. Okada, and T. Murata, Development of auto-detection method of lower cut-off frequency in magnetospheric plasma wave spectrum (IEICE (in Japanese) in press)
- Tokunaga T., Akimasa Yoshikawa, Teiji Uozumi, Kiyohumi Yumoto, and MAGDAS/CPMN Group, An application of Independent Component Analysis to Pi 2 magnetic pulsations observed on the ground-Blind Source Deconvolution, 124th SGEPS Fall Meeting, Sendai, Japan, Oct. 9-12, 2008.
- Tsubouchi, K., Alfvén wave evolution in a corotating interaction region, ICPP2008, Sep.8-12, 2008, Fukuoka, Japan.

Conferences and Meetings (August 2008 ~ February 2009)

- 1) XXIXth URSI General Assembly, Chicago, USA Aug. 9-16, 2008
- 2) IMAS/The International Radiation Symposium (IRS2008): Current Problems in Atmospheric Radiation, Brazil Aug. 3-8, 2008
- 3) ICPP2008 : International Congress on Plasma Physics, Fukuoka, Japan Sep. 8-12, 2008
- 4) BepiColombo/(Messenger) Science Working Team Meeting #3, Sendai, Japan Sep. 16-18, 2008
- 5) SGEPS Fall Meeting, Sendai, Japan Oct. 9-12, 2008
- 6) European Microwave Week (EuMW) 2008, Amsterdam, Netherlands Oct. 27-31, 2008
- 7) International Symposium on Antennas , Propagation and Em Theory (ISAPE) 2008, Kunming, China, Nov. 2-6, 2008
- 8) 1st International Symposium of Polar Research, Tokyo, Japan Nov. 4-6, 2008
- 9) International Symposium: Fifty Years after IGY -Modern Information Technologies and Earth and Solar Sciences-, Tokyo, Japan, Nov. 10-13,
- 10) 2008 ULTIMA (Ultra Large Terrestrial International Magnetometer Array) General Meeting, Tsukuba, Japan, Nov. 13, 2008.
- 11) The 15th world congress on Intelligent Transport Systems (ITS) 2008, New York Nov. 16-20, 2008
- 12) AGU 2008 Fall Meeting, San Francisco Dec. 15-19, 2008
- 13) Asia-Pacific Microwave Conference (APMC) 2008, Hong Kong and Macau Dec. 16-20, 2008

The ICPP (International Congress on Plasma Physics) 2008 meeting was held in Fukuoka, Japan, on Sep. 8-12, 2008. This meeting covered a wide area of plasma physics, including ULF waves, thus many papers were presented related to ULF waves.

The 118th SGEPS (Society of Geomagnetism and Earth, Planetary and Space Sciences) Fall Meeting was held in Sendai, Japan, on Oct. 9-12, 2008. This meeting covered a wide area of geomagnetism and earth, planetary and space sciences, including ULF waves, thus many papers were presented related to ULF waves.

The 2008 ULTIMA General Meeting was held in Tsukuba, Japan, On Nov. 13, 2008. ULTIMA (Ultra Large Terrestrial International Magnetometer Array) is an international consortium that aims at promoting collaborating research on the magnetosphere, ionosphere, and upper atmosphere through the use of ground-based magnetic field observations. ULTIMA is composed of individual magnetometer arrays in different countries/regions. The official webpage of ULTIMA is at: <http://www.serc.kyushu-u.ac.jp/ultima/ultima.html> At the 2008 ULTIMA General meeting, several presentations were made on ULF waves observed by the magnetometer arrays.

Future Conferences and Meeting

- 1) 3rd European Conference on Antenna and Propagation (EuCAP) 2009, Berlin March 23-27, 2009
- 2) IEEE MTT-S International Microwave Symposium 2009, Boston Massachusetts June 7-12, 2009
- 3) IEEE AP-S 2009, Charleston, South Carolina May 31-June 6, 2009
- 4) Modern Challenges in Nonlinear Plasma Physics: A conference honoring the career of Dennis Papadopoulos" June 15-19, 2009, Sani Resort, Halkidiki, Greece
<http://www.astro.auth.gr/~vlahos/kp>
- 5) The 11th Scientific Assembly of IAGA, Hungary Aug. 23-30, 2009
- 6) JInternational Symposium on Antenna Technology and Applied Electromagnetics (ANTEM) and the Canadian Radio Sciences Meeting (URSI/CNC), Banff, Canada uly 27-30, 2009
- 7) IEEE AP-S 2010, Toronto, Ontario, Canada July 10-17, 2010

Acknowledgement

The editors thank to Dr. H. Kojima, Dr. Y. Kasahara, Dr. S. Yagitani, Dr. H. Kawano, Dr. Y. Miyoshi, Dr. A. Kumamoto, and Dr. K. Ishisaka for their contribution to this report.